# Photonic upconversion maximization for nonlinear meta-material enabled by deep learning

Lakshmi Raju*[a], Zhaocheng Liu [a], Dayu Zhu [a], Andrew Kim [a], Ekaterina Poutrina[bc], Augustine Urbas[c], Wenshan Cai [ad]

[a]School of Electrical and Computer Engineering, Georgia Institute of Technology, Atlanta, GA 30332, USA;

[b]UES, Inc, 4401 Dayton-Xenia Rd, Dayton, OH 45432, USA;

[c]Air Force Research Laboratory, Wright-Patterson Air Force Base, Dayton, Ohio 45433, USA;

[d]School of Materials Science and Engineering, Georgia Institute of Technology, Atlanta, GA 30332, USA

## ABSTRACT

Photonic upconversion from the infrared regime to the visible spectrum can occur through sum-frequency generation (SFG). A second-order nonlinear optical response, such as SFG, can be produced from a nonlinear material, in this case an ABC nanolaminate. Optimization of a metamaterial consisting of a plasmonic nanolaminate device can maximize the SFG from incident wavelengths. Utilization of a deep learning framework removes the need for traditional guess and check methods and creates new possibilities for plasmonic geometries. Applications of this research include low-cost night vision or low light imaging systems for defense, autonomous vehicles, and other commercial uses.

**Keywords:** nanophotonics, metamaterial, nonlinear, optics, deep learning, plasmonics, upconversion

## 1. INTRODUCTION

### Nonlinear Optics

It can be said that linear optics is noticed as a child – looking in a mirror and seeing a reflection, or when searching for the pot of gold at the end of a rainbow. Linear optics is displayed all around us, and thereby makes it much easier to grasp as it can be simply demonstrated for the most general cases of refraction, reflection, and diffraction.

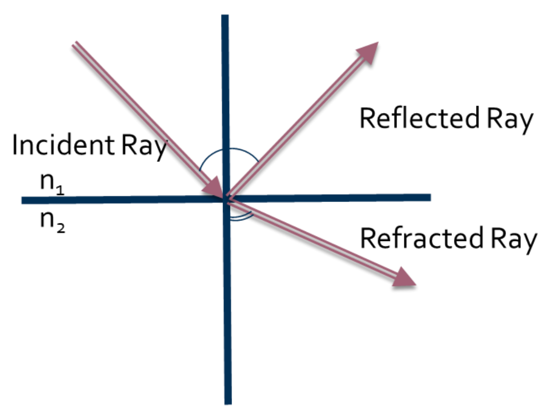


Figure 1. Example of linear optics where an incident ray in a material with a refractive index of n1 hits the surface with a refractive index of $n_2$. This results in a reflected ray and a refracted ray.

We can describe a linear optical response as one where monochromatic light entering a linear system maintains its frequency, an example of which is in Figure 1. While the light may be delayed, polarized, or otherwise acted upon, its frequency will remain unchanged. It is important to note that in a linear case, the refractive index is related to the linear susceptibility, or $\chi^{(1)}$, which can further be elucidated as such: $n = \sqrt{\chi^{(1)} + 1}$.

Nonlinear Frequency Generation and Conversion: Materials and Devices XXII,
edited by Peter G. Schunemann, Proc. of SPIE Vol. 12405, 124050F

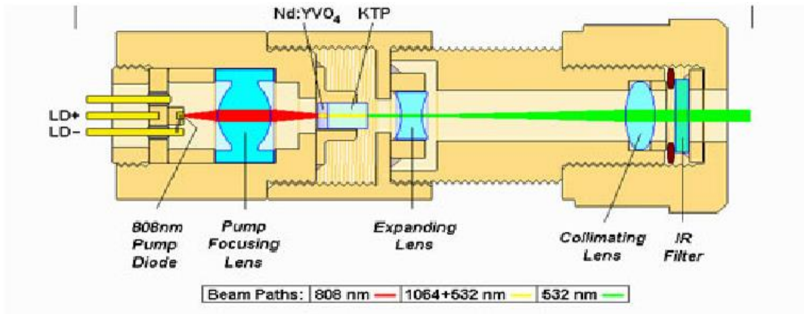


Figure 2. Image illustrating how a green laser pointer functions [1].

On the other hand, nonlinear optics is much more complex, and in most scenarios, the processes can't be visualized without an expensive or complex setup. Even a simple example of how a green laser pointer works, relies on trust and imagination between the teacher and audience as shown in Figure 2. It is a much more hidden process.

Nonlinear optics can be described as frequency mixing processes. Frequency mixing processes that occur dur to the applied electric field interacting with the nonlinear properties of a material allow for the generation of radiation at different frequencies.

A nonlinear material can have a nonlinear susceptibility, for example the second order nonlinear susceptibility would be referred to as $\chi^{(2)}$. More specifically, these nonlinear susceptibilities are tensors, so we would refer to the 2nd order susceptibility as $\chi_{ijk}^{(2)}$, where $i, j,$ and $k$ are the cartesian components of the field[2].

It is possible to reduce the tensor components to a contracted notation for simplicity.

$$d_{ijk} = \frac{1}{2}\chi_{ijk}^{(2)} \tag{2.1}$$

This can further be simplified using Kleinman's symmetry to assume $d_{ijk}$ is symmetric in the last two indices, leading to $d_{ijk} = d_{il}$[2]. Where:

$$\begin{array}{lcccccc} jk: & 11 & 22 & 33 & 23,32 & 31,13 & 12,21 \\ l: & 1 & 2 & 3 & 4 & 5 & 6 \end{array}. \tag{2.2}$$

Leading to a 3 × 6 nonlinear susceptibility tensor:

$$d_{il} = \begin{bmatrix} d_{11} & d_{12} & d_{13} & d_{14} & d_{15} & d_{16} \\ d_{21} & d_{22} & d_{23} & d_{24} & d_{25} & d_{26} \\ d_{31} & d_{32} & d_{33} & d_{34} & d_{35} & d_{36} \end{bmatrix}. \tag{2.3}$$

Using the contracted notation, we can describe the nonlinear polarization of second-harmonic generation as such:

$$\begin{bmatrix} P_x(2\omega) \\ P_y(2\omega) \\ P_z(2\omega) \end{bmatrix} = 2\epsilon_0 \begin{bmatrix} d_{11} & d_{12} & d_{13} & d_{14} & d_{15} & d_{16} \\ d_{21} & d_{22} & d_{23} & d_{24} & d_{25} & d_{26} \\ d_{31} & d_{32} & d_{33} & d_{34} & d_{35} & d_{36} \end{bmatrix} \begin{bmatrix} E_x(\omega)^2 \\ E_y(\omega)^2 \\ E_z(\omega)^2 \\ 2E_y(\omega)E_z(\omega) \\ 2E_x(\omega)E_z(\omega) \\ 2E_x(\omega)E_y(\omega) \end{bmatrix}. \tag{2.4}$$

Generally, the way that the elements of nonlinear susceptibility tensors are calculated are by first identifying the nonvanishing elements and their symmetries based on the crystalline structure of the material. Then the nontrivial elements are experimentally measured.

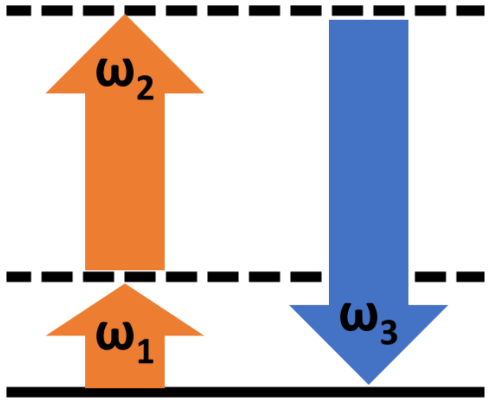


Figure 3. Energy level description of sum-frequency generation. Two photons of frequencies ω1 and ω2 combine to form a photon of frequency $\omega_3 = \omega_1 + \omega_2$.

**Sum Frequency Generation**

Second-harmonic generation is a specific case of sum-frequency generation (SFG). In second-harmonic generation, two photons of the same frequency, $\omega$, are effectively combined to form a single photon of double the frequency, $2\omega$. We can say the second-harmonic generation is a process where $\omega + \omega \rightarrow 2\omega$, when interacting with a nonlinear material. In sum-frequency generation, two photons of different frequencies, $\omega_1$ and $\omega_2$, interact to result in the formation of a photon with a frequency of the sum of the two photons, $\omega_3 = \omega_1 + \omega_2$ as shown in Figure 3. The nonlinear polarization, $P(\omega_1 + \omega_2) = 2\varepsilon_0\chi^{(2)}E(\omega_1)E(\omega_2)$, further shows the similarity to the second-harmonic generation.

The full nonlinear polarization for sum-frequency generation, in the contracted notation, is as follows,

$$\begin{pmatrix} P_x(\omega_1+\omega_2) \\ P_y(\omega_1+\omega_2) \\ P_z(\omega_1+\omega_2) \end{pmatrix} = \begin{pmatrix} P_x(\omega_3) \\ P_y(\omega_3) \\ P_z(\omega_3) \end{pmatrix} = \epsilon_0 \begin{pmatrix} d_{11} & d_{12} & d_{13} & d_{14} & d_{15} & d_{16} \\ d_{21} & d_{22} & d_{23} & d_{24} & d_{25} & d_{26} \\ d_{31} & d_{32} & d_{33} & d_{34} & d_{35} & d_{36} \end{pmatrix} \begin{pmatrix} E_x(\omega_1)E_x(\omega_2) \\ E_y(\omega_1)E_y(\omega_2) \\ E_z(\omega_1)E_z(\omega_2) \\ E_y(\omega_1)E_z(\omega_2) + E_z(\omega_1)E_y(\omega_2) \\ E_x(\omega_1)E_z(\omega_2) + E_z(\omega_1)E_x(\omega_2) \\ E_x(\omega_1)E_y(\omega_2) + E_z(\omega_1)E_y(\omega_2) \end{pmatrix} \quad (2.5)$$

, and can be simplified for the ABC nanolaminate as follows,

$$\begin{gathered} \boldsymbol{P_x}(\omega_1+\omega_2) = \boldsymbol{\epsilon_0\chi_{xxz}}[E_x(\omega_1)E_z(\omega_2) + E_z(\omega_1)E_x(\omega_2)] \\ \boldsymbol{P_y}(\omega_1+\omega_2) = \boldsymbol{\epsilon_0\chi_{xxz}}[E_y(\omega_1)E_z(\omega_2) + E_z(\omega_1)E_y(\omega_2)] \\ \boldsymbol{P_z}(\omega_1+\omega_2) = \boldsymbol{\epsilon_0\chi_{zxx}}\big[E_x(\omega_1)E_x(\omega_2) + E_y(\omega_1)E_y(\omega_2)\big] + \boldsymbol{\epsilon_0\chi_{zzz}}[E_z(\omega_1)E_z(\omega_2)] \end{gathered} \quad (2.6)$$

from these equivalencies, $\chi_{xxz} = d_{15} = d_{24}$, $\chi_{zxx} = d_{31} = d_{32}$, and $\chi_{zzz} = d_{33}$ [2, 3].

Utilizing the physics of sum-frequency generation, a process of photonic upconversion can take place. In nonlinear optics, upconversion is described as sum-frequency generation. Two, or more, photons are absorbed, and a photon of a shorter wavelength is emitted. This frequency mixing allows for the detection of light otherwise unable to be counted using available imaging processes. Sum-frequency generation is most utilized in spectroscopy, developed for the use of studying interfaces such as gas-liquid interfaces.

In this research, sum-frequency generation is used for photonic upconversion in order to convert infrared light to the visible regime. This research has many very important applications. One important application for SFG upconversion of near infrared signals is for low-cost night vision/low light imaging systems. The uses for these imaging systems range from defense applications to autonomous vehicles and more.

SFG requires two incident beams of light, so the set up can be described as a pump-probe system. In this scenario, two infrared incident light sources – one of significance to be converted, and the other for the upconversion process, are focused on a nonlinear material such as an ABC nanolaminate. The resulting light in the visible regime would then be collected. For the ABC nanolaminate to be used as a nonlinear metamaterial, a plasmonic structure is required, in order to take advantage of the surface plasmon effect, as explained earlier.

Utilizing a deep learning framework, consisting of a pattern generator and a simulator, the geometry of the plasmonic device can be optimized, thereby optimizing the strength of the emitted visible light from the metamaterial allowing for more efficient SFG upconversion.

**Deep Learning**

The most important portion of a deep learning framework used to optimize a pattern for an optical response is the pattern generator. The pattern generation allows for the creation of geometries outside the traditional scope. To widen the possible geometries possible from the pattern generator, we build upon the existing Compositional Pattern-producing Network (CPPN). A CPPN is essentially an ANN with genetic algorithms.

The possibilities of complex CPPNs were highlighted in 2006 by K. Stanley, and it's use has only skyrocketed since then[5]. ANNs can be used to perform the classification of data with multiple layers of artificial neurons. CPPNs are a version of ANNs that also use genetic algorithms as an evolution method[6].

In order to truly understand the idea behind CPPNs, some background on activation functions is required. The way that ANNs work depends on artificial neurons. In ANNs, an activation function allows for the 'learning' of complicated patterns that might occur in the data. This is crucial for deep learning applications to be able to 'learn' and more importantly 'create' or 'identify' from patterns that humans can't easily find in large and complex data sets.

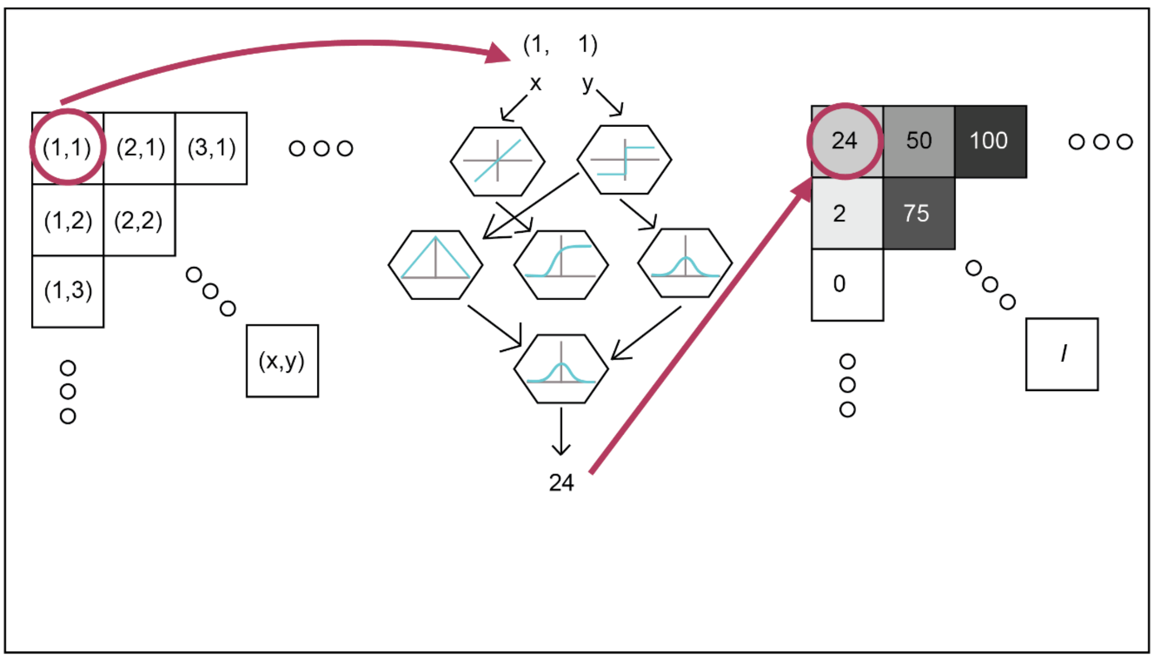


Figure 4. Compositional Pattern Producing Network Architecture. The CPPN works by defining the image canvas into a grid of pixels with coordinates. Each pixel is then run through the CPPN and an intensity value is output. This is repeated for each pixel leading to a canvas full of generated intensities, in other words, an image.

Activation functions add nonlinearities to networks, letting the networks essentially do more complex procedures. These functions effectively determine the neural network output using equations. These equations range from step and sigmoid functions to hyperbolic tangents and the identity function. Some examples of activation function plots are shown in Figure 4 in the CPPN architecture.

This collective use of varied activation functions leads to the naming of CPPNs – *compositional* pattern-producing networks. This also allows for the infinite number of possible geometries as the results can be sampled at any resolution.

Practically speaking, in this research, CPPNs permit the generation of both single and multi-unit geometric structures for the plasmonic pattern.

## 2. RESULTS

The objective of the sum-frequency generation research is to expand upon the demonstrated ability to optimize materials for linear optical responses and a nonlinear second harmonic optical response to other linear and nonlinear optical responses and advance the current data learning framework.

The purpose of this device is to upconvert a near infrared (NIR) signal to the visible regime. This research has many very important applications. Using a lab fabricable nonlinear metamaterial such as the ABC nanolaminate decreases the cost and thickness of the device. Such as easy to fabricate device can also be easily manufactured.

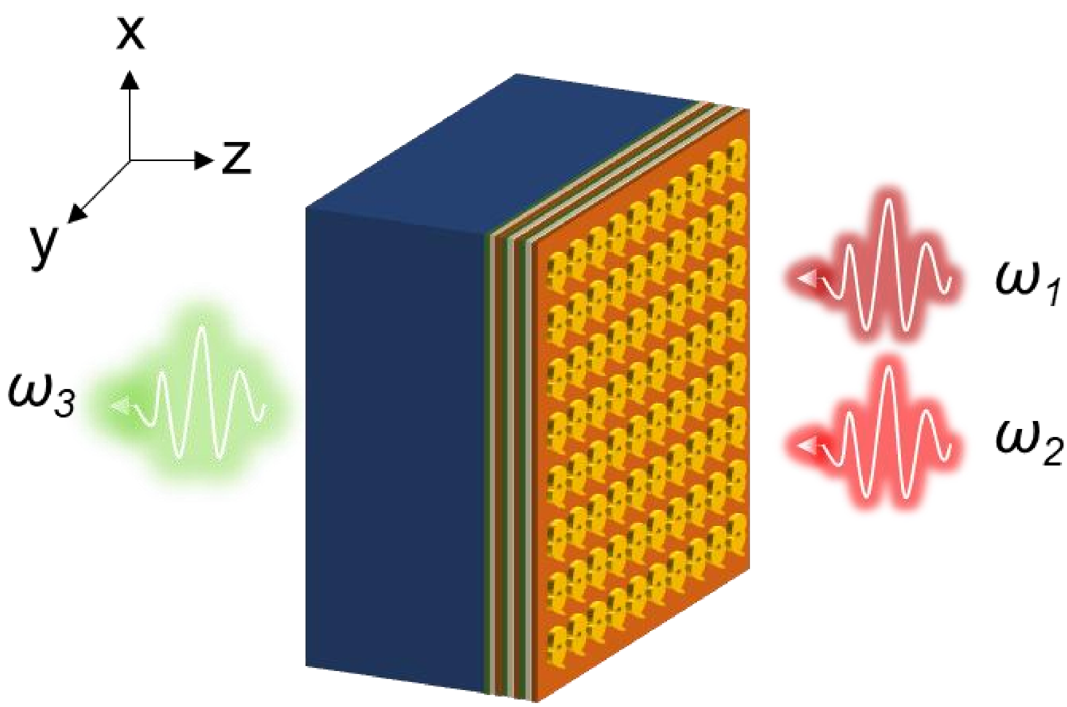


Figure 5. Illustration of SFG nonlinear metamaterial device. The schematic shows the ABC nanolaminate with a periodic plasmonic structure atop. The incident infrared light, $\omega_1$ and $\omega_2$, is normal to the surface of the metamaterial device. The plasmonic structures here generate a z-component of electric field, allowing the ABC nanolaminate to emit visible light, $\omega_3$ through sum-frequency generation. The nanolaminate is comprised of three periodic layers, $TiO_2$, $Al_2O_3$, and $HfO_2$ and the plasmonic structure is patterned above the nanolaminate.

### 2.1. SFG Nonlinear Metamaterial Parameters

The device parameters are as follows, periodicity, $p = 380\ nm$, ABC nanolaminate thickness, $t_{ABC} = 75\ nm$, gold plasmonic thickness, $t_{Au} = 45\ nm$, incident IR wavelengths, $\lambda_1 = 800\ nm$ and $\lambda_2 = 1550\ nm$, output wavelength, $\lambda_3 = 528\ nm$. A schematic of the device is shown in Figure 5.

Once the device parameters are finalized, the full-wave simulation of sum-frequency generation in such a device was created. In this instance, Comsol was used as the full-wave simulation software. The full-wave simulation was validated in a number of ways, but most importantly by comparing the results of the sum-frequency generation simulator with the same parameters of the second-harmonic generation device.

As earlier described, SHG is a special case of SFG, where both incident frequencies are identical, and the output is double the incident frequency.

The general framework for this work, focused on SFG, requires a pattern generation network and simulator network[4]. Given the SFG nonlinear metamaterial parameters, utilizing a pattern generator and simulator, we can find an optimal plasmonic geometry for the device to maximize the sum-frequency generation.

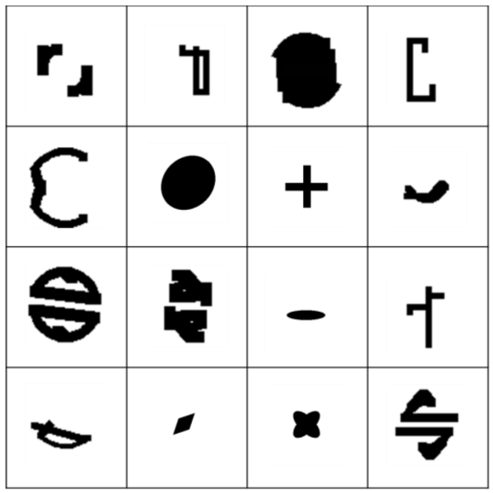

Figure 6. Sample of patterns used as training data for CPPN. 10,000 patterns were used to train the CPPN or pattern generator.

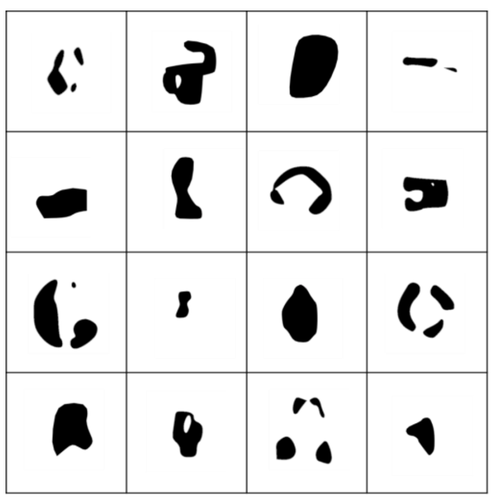

Figure 7. Randomly generated patterns from CPPN. A variety of single and multi-unit geometries can be seen. There are also patterns that contain ‘holes’ that were not present in the patterns generated by the VAE. All of these show the increase in possible geometries when using the CPPN architecture for pattern generation.

For the maximization of SFG in our device, the CPPN pattern generator is crucial. Figure 6 shows a sample of patterns used to train the CPPN, and Figure 7 shows a sample of randomly generated patterns from the CPPN.

Once the pattern generator was created, then a deep learning simulator could be used to simulate the sum-frequency generation for any plasmonic geometry atop our nonlinear metamaterial. A simulator based on ResNet18 architecture, was created.

### 2.2. SFG Optimization

To train the simulator, 10,000 patterns were randomly generated from the CPPN. Then those patterns were input into the full-wave simulator to produce what will be called 'actual' SFG values. Both the patterns and corresponding SFG values are then used for training and validation of the simulator.

Given a randomly generated pattern for the plasmonic structure, the simulator can predict the SFG. The last step is optimization. Utilizing an Evolution Strategy, through a process of selection, reproduction, and mutation, the simulator can be modified to output a pattern for a particular SFG value [5].

Figure 8. Results from Evolution Strategy for optimal plasmonic geometry to yield maximal SFG response.

For instance, searching for a pattern that does not lead to a second-harmonic response would lead to a completely covered canvas indicating a gold mirror would be the plasmonic device. Figure 8 shows the results for a maximal SFG response for the plasmonic ABC nanolaminate device. All four patterns look similar but do have minor variations.

Figure 9. Optimized structure and split ring resonator (SRR) with similar parameters. The optimized structure had a significantly higher second-harmonic nonlinear optical response as compared to the split ring resonator.

To show that the optimal result is indeed due to the unusual shape, and not the resemblance to a split ring resonator (SRR), a similarly shaped split ring resonator was simulated in a full-wave simulator to compare the results, as shown in Figure 9. The SRR had an SFG value two orders of magnitude less than the optimal shape.

## 3. CONCLUSION

In summary, the results of the research could be furthered for other nonlinear optical responses. As other second-order nonlinear responses, physics-wise, are similar to sum-frequency generation, it seems that the deep learning framework can be used as-is simply with new training, for those responses. The framework can also be expanded for other order nonlinear responses such as third order responses. As long as a full-wave simulation can be created for the nonlinear optical response, this framework can be used to optimize a corresponding plasmonic nonlinear metamaterial device.

This research expands the scope of possible devices for optical phenomena. With the plasmonic ABC nanolaminate combined with the deep learning framework, applications include, but are not limited to, integrated optics, CMOS technology, low-cost lowlight/night vision for autonomous vehicles and defense application.

Not only does this enable the optimization of devices, but also generates patterns that one would not think of. The possible efficiency improvement of devices is something that could transform current optical devices. With the future advancements in machine learning, the concepts and results of this research could develop into even more efficient frameworks for designing advanced devices for virtual reality, bio-photonics, integrated semiconductor devices and more.

## ACKNOWLEDGEMENTS

This work was supported in part by the National Science Foundation under Grant No. DMR-2004749, and by the Office of Naval Research under Grant No. N00014-17-1-2555. L.R. acknowledges the support of the National Science Foundation Graduate Research Fellowship under Grant No. DGE-1650044. The authors are grateful for the support of the AFRL Minority Leadership – Research Collaboration Program and TOPS V Program, ForWarD to Materials Data Science and Informatics (FWD-MDSI), administered by ARCTOS Technology Solutions (formerly Universal Technology Corporation) under Task Order FA8650-19-F-5830 (TO 0005).

## REFERENCES

[1] E. Garmire, "Nonlinear optics in daily life," Optics express, 21, 30532-44 (2013).
[2] R. W. Boyd, [Nonlinear optics] Academic Press, Amsterdam ; Boston(2008).
[3] A. Hermans, C. Kieninger, K. Koskinen *et al.*, "On the determination of $\chi(2)$ in thin films: a comparison of one-beam second-harmonic generation measurement methodologies," Scientific Reports, 7(1), 44581 (2017).
[4] L. Raju, K.-T. Lee, Z. Liu *et al.*, "Maximized Frequency Doubling through the Inverse Design of Nonlinear Metamaterials," ACS Nano, 16(3), 3926-3933 (2022).
[5] K. O. Stanley, "Exploiting Regularity Without Development."
[6] K. Ghaderi, F. Akhlghian, and P. Moradi, "A new digital image watermarking approach based on DWT-SVD and CPPN-NEAT." 12-17.